

Durham Research Online

Deposited in DRO:

18 November 2014

Version of attached file:

Accepted Version

Peer-review status of attached file:

Peer-reviewed

Citation for published item:

Xu, T. and Morris, T. A. and Szulczewski, G. J. and Metzger, R. M. and Szablewski, Marek (2002)
'Current-voltage characteristics of an LB monolayer of didecylammonium tricyanoquinodimethanide measured between macroscopic gold electrodes.', *Journal of materials chemistry*, 12 (10). pp. 3167-3171.

Further information on publisher's website:

<http://dx.doi.org/10.1039/b203789k>

Publisher's copyright statement:

Additional information:

Use policy

The full-text may be used and/or reproduced, and given to third parties in any format or medium, without prior permission or charge, for personal research or study, educational, or not-for-profit purposes provided that:

- a full bibliographic reference is made to the original source
- a [link](#) is made to the metadata record in DRO
- the full-text is not changed in any way

The full-text must not be sold in any format or medium without the formal permission of the copyright holders.

Please consult the [full DRO policy](#) for further details.

Current-Voltage Characteristics of an LB Monolayer of di-Decylammonium Tricyanoquinodimethanide Measured between Macroscopic Gold Electrodes

Tao Xu, Todd A. Morris, Greg J. Szulczewski, and Robert M. Metzger*

*Department of Chemistry, The University of Alabama,
Tuscaloosa, Alabama 35487-0336, USA*

and

Marek Szablewski

*Department of Physics, South Road, University of Durham, Durham DH1
3LE, UK*

Abstract

Didecylammonium tricyanoquinodimethanide, a zwitterionic molecule in the type of $D^+-\pi-A^-$ (where D^+ = ammonium, π = ethylene "bridge", and A^- = tricyanoquinodimethanide), forms a Pockels-Langmuir monolayer film at the air-water interface. The molecules can be transferred quantitatively as a Langmuir-Blodgett (LB) monolayer onto a gold surface. Using the "cold-gold" evaporation technique, a set of several macroscopic gold electrode pads were evaporated atop the LB monolayer. Pads which had macroscopic defects were electrical short circuits, but across many pads finite electrical currents were observed as a function of applied bias; however, no obvious electrical rectification was found. The monolayer thickness on a gold substrate measured by XPS to be ~ 22 Å. Reflection-absorption infrared spectroscopy (RAIRS) indicates that the molecules have a preferred orientation in the film, but are not well ordered. Angle-resolved X-ray photoelectron spectroscopy (XPS) suggests that many of the molecules

are oriented anti-parallel to each other, possibly because dipole-dipole forces favor such an anti-parallel orientation. This latter observation helps to explain why no electrical rectification was found.

Introduction

The electrical current (I) through molecules as a function of applied voltage (V) has been investigated using a scanning tunneling microscope (STM) by setting a metallic tip above a molecular monolayer deposited on a conducting substrate [1, 2, 3], but the coupling between tip and molecule is often not stable [4, 5]. The potential drop through the molecule is much less than that between the STM tip and the bottom electrode. Much work has been done on “Al | monolayer | Al” sandwiches [6, 7], or “Al | monolayer | Hg” sandwiches [8], but the inevitable oxide layer has beclouded interpretation or raised some doubt whether the true properties of the monolayer were indeed measured. Stationary “Au | molecule monolayer | Au” sandwiches are useful devices for investigating the current-voltage (I-V) characteristics because the gold atoms and the molecules are in a stationary and hopefully ohmic contact [9]. These structures may be more practical molecular electronic devices. We recently demonstrated the electrical rectification (i.e. strongly asymmetrical I-V characteristics) in the $D^+-\pi-A^-$ molecule hexadecylquinolinium tricyanoquinodimethanide ($C_{16}H_{33}Q^+-3CNQ^-$, molecule **1**) measured between oxide-free gold electrodes, using the “cold gold” technique to prevent damage to the monolayer [10, 11]. We report here the I-V characteristics, measured between gold electrodes, of a Langmuir-Blodgett (LB) monolayer of another $D^+-\pi-A^-$ molecule, didecylammonium tricyanoquinodimethanide, $(C_{10}H_{21})_2N^+-3CNQ^-$ (molecule **2**) (Figure 1), which has a

structure formally similar to that of **1**. No rectifying current was observed, probably because the monolayer has a significant amount of disorder, i.e. because many of the electrical dipoles are arranged antiparallel to each other.

Experimental Section

Synthesis

The $(\text{C}_{10}\text{H}_{21})_2\text{N}^+-3\text{CNQ}^-$ zwitterion was synthesized via *in situ* enamine formation [12]. Didecylamine (0.729 g, 0.253 mL, 2.45 mmol) was stirred under nitrogen in dry dichloromethane (150 mL) at room temperature with an excess of anhydrous sodium sulfate for half an hour. Subsequently, acetaldehyde (0.107 g, 0.137 mL, 2.45 mmol) was added dropwise as a solution in dichloromethane (10 mL). The solution was stirred with gentle heating for 40 min and then a solution of TCNQ (0.5 g, 2.45 mmol) in warm dichloromethane (175 mL) was added dropwise. The reaction mixture was stirred with heating at the reflux temperature for 18 hours. During this time the reaction mixture exhibited a color change from yellow to green. After three hours, the color had changed to turquoise and finally to blue. A UV/Vis absorption spectrum of the reaction mixture showed the characteristic peaks associated with a zwitterionic species. The blue solution was removed from the heat and filtered under gravity to remove sodium sulfate from the reaction mixture. The filtrate was evaporated to dryness *in vacuo*. The resultant solid was recrystallised from hot acetonitrile. The product was collected by filtration under suction and washed with ether 2 x (20 mL). The product $(\text{C}_{10}\text{H}_{21})_2\text{N}^+-3\text{CNQ}^-$ was obtained as metallic-like green-gold needle-like crystals (367 mg, 25% theoretical yield). ^1H NMR, (CD_2Cl_2), $\delta = 0.8 - 1.8$ ppm (multiplet, 38H,

-(CH₂)₃CH₃ x 2), δ = 3.45 ppm (dq, 4H, -CH₂- x 2), δ = 7.1 & 7.5 ppm (4H, doublet of doublets, p-substituted benzene ring), δ = 6.3 ppm (d, 1H, H-C=C-H), δ = 7.8 ppm (d, 1H, H-C=C-H [proton nearest positively charged N]). Mass spectrum: m/z, M⁺ 500. (100%, molecular ion), melting temperature 159.6-161.2°C. Calc. for C₃₃H₄₈N₄: C, 79.15%; N, 11.19%; H, 9.66%. Found: C, 78.68%; N, 11.44%; H, 9.50%.

Preparation of Bottom Gold Electrode

In a clean room, glass substrates (Corning 1747F) or Si (111) substrates (for XPS measurements) were cleaned by first rinsing with acetone for 2 minutes, and then with 2-propanol for 2 minutes in an ultrasonic bath, followed by drying in a stream of dry nitrogen. Our evaporation chamber (Edwards E306 Evaporator) was pumped to a base pressure of 4×10^{-6} mbar using a liquid-nitrogen trapped diffusion pump. In the evaporation chamber, the substrates were held with stainless-steel clips onto a copper plate that contained a halogen lamp heater and a platinum resistance thermometer. Before a deposition, the sample holder and the substrates were preheated to 260°C in vacuum for at least 6 hours. After briefly outgassing a Ti wire, a 7 nm Ti adhesion layer was evaporated onto the heated glass or Si (111) substrates at a rate of 0.05 nm s⁻¹. Then, without breaking the vacuum, 150 nm Au were evaporated onto the Ti from a Mo evaporator boat at 0.02 nm s⁻¹. During the evaporation, the pressure remained below 6×10^{-6} mbar. After evaporation, the samples were annealed for another 6 hrs at 260°C, and were then cooled to room temperature in vacuum. The thickness of the films was measured with a quartz crystal thickness monitor. Fig. 2 shows a typical AFM image of the Au film prepared under the above conditions.

LB-Film Deposition

The Au substrates were cleaned by UV light in a stream of ozone (JeLight Co., Inc. Model 42) for 80 seconds and immediately immersed into deionized pure water. The $(C_{10}H_{21})_2N^+-3CNQ^-$ zwitterion was spread from dichloromethane onto pure water (18.3 M Ω cm). The surface pressure-area isotherm is shown in Fig.3. The monolayer collapses between $\pi_c = 39$ and 41 mN·m⁻¹. At the air-water interface, a monolayer of $(C_{10}H_{21})_2N^+-3CNQ^-$ was transferred onto the Au film on the upstroke at 32 mN·m⁻¹. The transfer ratios were slightly greater than unity (1.01 to 1.03), due to partial surface roughness. The samples were then desiccated in a vacuum over P₂O₅ for 72 h.

Deposition of Top Gold Electrodes by "Cold Gold Evaporation"

The melting point of Au is 1337 K, at which temperature the kinetic energy of a gold atom is $(3/2) k_B T = 0.17$ eV. In a conventional direct evaporation procedure, short circuits were always formed even when the sample sits atop a Cu plate cryocooled to 77 K or when the distance from boat to sample was increased from 50 cm to 150 cm [13]. Most likely, the evaporated gold atoms penetrate into the monolayer [14] and the heat radiation from the boat also causes damage [15]. In the cold gold evaporation, all the samples were placed on a copper plate cooled by liquid nitrogen, and all the samples faced away from the boat. This also prevents radiation from the boat reached the LB monolayer. The evaporation chamber was first evacuated to 4×10^{-6} mbar, purged for one hour with an Ar pressure of 1×10^{-3} mbar, then maintained at an Ar pressure of 1×10^{-3} mbar. Gold was evaporated from a Mo boat at a nominal rate of 0.02 nm s⁻¹ for the first 200 nm, and then at 0.1 nm s⁻¹ for the next 400 nm. Due to the Ar, Au atoms must

collide several times with Ar atoms before reaching the substrate and lose kinetic energy in each collision. The temperature of the Au vapor near the LB film was measured (Templabel) to be below 363 K [11]. The Au pads that formed through the holes in the contact mask were measured by a profilometer to be 17 nm thick. The thickness was much less than the nominal thickness of 600 nm recorded by the quartz crystal monitor (which is line-of-sight with the evaporation). This technique provided many pads that were not electrically shorted.

Current-Voltage Measurements

A voltage source (Hewlett-Packard model 3245A) and a multimeter (Hewlett-Packard model 3457A) were connected by a National Instruments IEEE-488 GPIB interface to a Gateway 2000 model P5-60 microcomputer. The multimeter, sample, and all signal lines, except for some low-impedance high-level lines, were enclosed in a Faraday cage. The interval between successive data points was 3 seconds, during which the source did not apply a voltage to the sample. Each I-V measurement took 1 second, to allow a stable current to be read. As shown in Fig. 4, contact to the bottom Au electrode was achieved using a Ga/In eutectic droplet. A Ga/In droplet at the end of a tinned flexible wire was positioned onto the top Au pad using a micromanipulator. When the top Au electrode is positively biased, the voltage is considered to be positive.

Infrared Spectroscopy

Reflection-absorption infrared spectra (RAIRS) were measured on a Nicolet Magna-IR 560 ESP Spectrometer with a liquid nitrogen-cooled mercury cadmium

telluride wide-band detector. The resolution was set to 2 cm⁻¹. The incident angle of the p-polarized light was set to 85° relative to the surface normal. A gold surface (150 nm thick), prepared in the same batch as the one with the organic monolayer on it, was cleaned by UV/ozone exposure for 80 seconds. For each spectrum, 1024 scans were averaged and ratioed to the clean gold surface.

The IR spectrum of bulk (C₁₀H₂₁)₂N⁺-3CNQ⁻ was recorded on a Bio-Rad FTS-40 FTIR infrared spectrophotometer, purged with dry N₂, at a resolution of 2 cm⁻¹. A concentrated solution of **2** in CH₂Cl₂ was dropped onto a KBr disk and dried in N₂ until no C-Cl stretch mode could be detected. The baseline was established by comparison to a clean KBr disk. For each spectrum, 128 scans were averaged, and the spectrum was ratioed to the clean KBr disk.

X-ray Photoelectron Spectroscopy

X-ray photoelectron spectra (XPS) were acquired on a Kratos Analytical Axis 165 Scanning Auger/XPS spectrometer. Mg K_α x-ray photons (1253.6 eV) were used as the exciting radiation. For the high-resolution XPS and sputter depth profile, a magnetic lens was chosen. For angle-resolved XPS, an electrostatic lens was used instead. To avoid systematic errors in the measurements, the take-off-angle (TOA) was selected in a random sequence of angles, rather than in an order of monotonically increasing (or decreasing) angles.

Results and Discussion

We have reported the electrical rectification of LB monolayer of hexadecylquinolinium tricyanoquinodimethanide ($C_{16}H_{33}Q^+-3CNQ^-$) measured between oxide-free gold electrodes [10, 11]. The rectification was explained by a modified Aviram-Ratner mechanism, which involves a transition from the ground zwitterionic state, with the large dipole moment of 43 D, to an electronic excited state with a smaller dipole moment of 8-11 D [6, 16].

The molecule $(C_{10}H_{21})_2N^+-3CNQ^-$ studied here is also a ground-state zwitterionic $D^+-\pi-A^-$ molecule. Fig.5 shows a high-resolution N(1s) core-level spectra of a $(C_{10}H_{21})_2N^+-3CNQ^-$ LB 12 multilayer on gold. The shoulder peak at a binding energy of 402.6 eV is ascribed to the positively charged ammonium nitrogen (as in ammonium salts, e.g., $N^+H_4NO_3$ at 402.3 eV [17]). The main peak at 399.6 eV is due to the negatively charged nitrogens in $C\equiv N$ groups (as in ionic salts such as KCN [18]).

Given the structure of the molecule, we expected to see electrical rectification through the LB monolayer of this molecule. Figs.6-8 show typical I-V traces for an “Au | $(C_{10}H_{21})_2N^+-3CNQ^-$ LB monolayer | Au” sandwich. The trace is sigmoidal over the +1.5V to -1.5 V sweep. The rectification ratios, defined as $RR = [\text{max. forward current}] / [\text{max. reverse current}]$, are all below 2. Previous work with molecule **1** showed that any film showing a rectification ratio less than 2 is to be considered as not rectifying. By this criterion, no rectification was observed in the current-voltage (I-V) characteristics of molecule **2**.

If the molecules in the LB film are in an orientation such that the molecular dipole moment is perpendicular to the applied electric field, then the I-V characteristics would not be rectifying [19]. Fig. 9 shows the Au(4f) region before and after sputtering away the $(C_{10}H_{21})_2N^+-3CNQ^-$ LB monolayer. The inset shows the C(1s) region. The film thickness (for a TOA of 90°) can be determined from the equation $d = -\lambda \ln(I_d/I_0)$, where d is the LB monolayer thickness, λ is the mean free path of the Au(4f) photoelectron, I_d is the Au(4f) intensity with the LB monolayer present, and I_0 is the Au(4f) intensity after sputtering.

The mean free path of a Au(4f) photoelectron at $1253.6-88=1165.6$ eV is calculated to be $\lambda = 34$ Å [20]. Using the measured Au(4f) peak area and λ , we calculated the LB monolayer film thickness to be $d = 21.2$ Å. The calculated length of the fully extended molecule is approximately 25 Å (CACHe), so the measured film thickness implies that the molecules in the LB monolayer are not aligned perpendicular on the gold surface. The tilt angle between the surface normal and molecular axis along the molecular dipole moment can be estimated to be about 32° .

Fig.10 shows the RAIRS of a $(C_{10}H_{21})_2N^+-3CNQ^-$ LB monolayer on Au and the peak frequencies are summarized in Table 1. The very intense peaks at 1193 cm^{-1} and 1568 cm^{-1} are most likely due to C-N and C=N stretches, respectively. These two peaks are very weak for molecule **1** [6] because of the ring effect. The intensities of the peaks due to C-N, C=N and C≡N stretches, relative to their intensities in the bulk (shown in Fig. 11), indicate that the molecules in the LB monolayer have a preferred orientation in the monolayer. The out-of-plane vibration mode of the two *o*- benzene hydrogens at 826 cm^{-1} indicates that the benzene ring cannot be lying parallel to the surface. The peak at

2927 cm^{-1} is due to CH_2 asymmetric stretch mode. In an all trans C-C alkane chain the CH_2 mode appears at 2920 cm^{-1} [21, 22]. The higher frequency for CH_2 asymmetric stretch mode indicates that the decyl chains are in a liquid-like phase [21, 22]. This is understandable, since the two decyl chains are bonded with the N atom in a "V" shape, and may have some difficulty in forming an ordered phase. The CH_3 asymmetric stretch mode at 2960 cm^{-1} indicates that the alkyl chain is not lying parallel to the surface, but extend away from the surface at some tilt angle.

Given the film thickness and RAIRS results, it is clear that the molecular transitional dipole moment in the LB monolayer are not parallel to the Au surface. The non-rectifying I-V characteristic can be explained by assuming that a large fraction of the molecules adopt an antiparallel alignment, resulting from the large dipole moment of $(\text{C}_{10}\text{H}_{21})_2\text{N}^+-3\text{CNQ}^-$ molecules and the insufficient hydrophobicity of a relatively short decyl chain. In the presence of the dipole interaction between zwitterionic molecules, a ten-carbon chain is not hydrophobic enough to force all the molecules in the monolayer to orient at the air-water interface so that the two decyl groups stick out of the water while the polar part remains in the water. Due to the strong dipole interaction between the molecules, it is very possible that for many of the molecules the positively charged ammonium is adjacent to the nearby negatively charged dicyanomethanide group (Fig.12). A similar phenomenon was observed in a secondary harmonic generation (SHG) and neutron reflectivity study by an LB monolayer of decylquinolinium tricyanoquinodimethanide ($\text{C}_{10}\text{H}_{21}\text{Q}^+-3\text{CNQ}^-$) at the air/water interface [23]. The balance between hydrophobic forces or dispersion (which favor all molecules to be oriented parallel to each other) and dipolar forces (which favor an antiparallel

arrangement) was not found for hexadecylquinolinium tricyanoquinodimethanide ($C_{16}H_{33}Q^+-3CNQ^-$), because the sixteen-carbon chain is long enough to make the hydrophobic interaction dominant.

Additional data to support the antiparallel dipole-dipole alignment is provided by angle-resolved XPS measurements on a $(C_{10}H_{21})_2N^+-3CNQ^-$ LB monolayer on Au (Fig. 13). With the decreasing take-off-angle, there is no apparent change in the relative intensity of the N atom in the ammonium group and the N in the three cyano groups. Thus, on average, the ammonium nitrogen and the cyano nitrogens are equally attenuated, which means that the $(C_{10}H_{21})_2N^+-3CNQ^-$ molecules in the LB monolayer are in some disordered arrangement. In contrast, in the angle-resolved XPS on an LB monolayer of $C_{16}H_{33}Q^+-3CNQ^-$ on gold, the intensity ratio of the quinolinium nitrogen to the cyano nitrogens increases with the decreasing take-off-angle, which indicates that the quinolinium nitrogen is above the three cyano groups, and that the monolayer is ordered [24].

Conclusions

The I-V curve through a LB monolayer of the ground-state zwitterionic molecule $(C_{10}H_{23})_2N^+-3CNQ^-$ was measured between oxide-free Au electrodes. The I-V curves are non-rectifying probably because of a partial or total antiparallel alignment of the molecules in the LB monolayer. The decyl chain is not hydrophobic enough to force all molecules into a parallel orientation at the air-water interface.

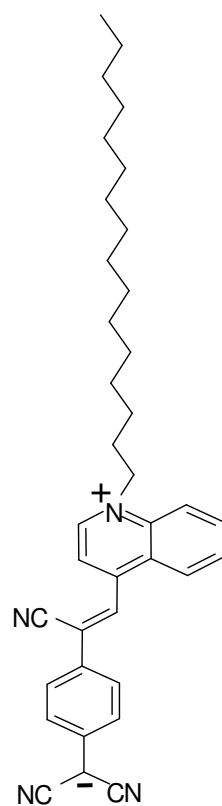
Acknowledgement

We are grateful to Dr. Shane C. Street and Dr. Earl Ada for stimulating discussions and technical support, and to the National Science Foundation (NSF DMR-0095235) for financial support.

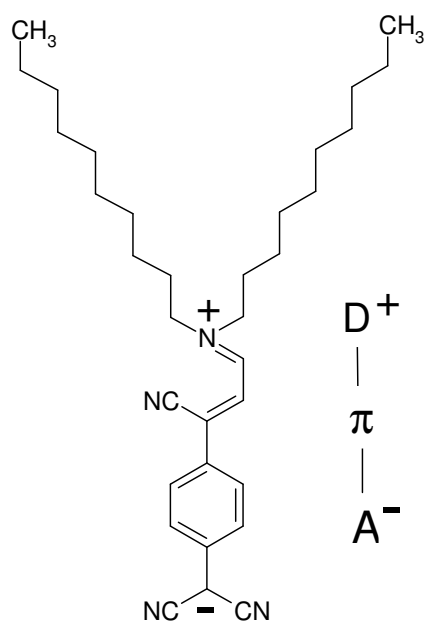
References

- [1] Aviram, A.; Joachim, C.; Pomerantz, M. *Chem. Phys. Lett.* **1998**, *146*, 490.
- [2] Han, W.; Durantini, E.; Moore, T. A.; Moore, A. L.; Gust, D.; Rez, P.; Leatherman, G.; Seely, G. R.; Tao, N.; Lindsay, S. M. *J. Phys. Chem.* **1997**, *101*, 10719.
- [3] Andres, R. P.; Bein, T.; Dorogi, M.; Feng, S.; Henderson, J. I.; Kubiak, C. P.; Mahoney, W.; Osifchin, R. G.; Reifengerger, R. *Science* **1996**, *272*, 1323.
- [4] Leatherman, G.; Druantini, E. N.; Gust, D.; Moore, T. A.; Moore, A. L.; Stone, S.; Zhou, Z.; Rez, P.; Liu, Y. Z.; Lindsay, S. M. *J. Phys. Chem. B*, **1999**, *103*, 4006.
- [5] Joachim, C.; Gimzewski, J. K.; Schlittler, R. R.; Chavy, C. *Phys. Rev. Lett.* **1995**, *74*, 2302.
- [6] Metzger, R. M.; Chen, B.; Hopfner, U.; Lakshmikantham, M. V.; Vuillaume, D.; Kawai, T.; Wu, X.; Tachibana, H.; Hughes, T. V.; Baldwin, J. W.; Hosch, C.; Cava, M. P.; Brehmer, L.; Ashwell, G. J. *J. Am. Chem. Soc.* **1997**, *119*, 10455.
- [7] Chen, B.; Metzger, R. M.; *J. Phys. Chem. B* **1999**, *103*, 4447.
- [8] Mann, B.; Kuhn, H.; *J. Appl. Phys.* 1971, *42*, 4398.
- [9] Chen, J.; Reed, M. A.; Rawlett, A. M.; Tour, J. M. *Science* **1999**, *286*, 1550.

- [10] Xu, T.; Peterson, I. R.; Lakshmikantham, M.; Metzger, R. M. *Angew. Chem. Int. Ed. Engl.* **2001**, *40*, 1749.
- [11] Metzger, R. M.; Xu, T.; Peterson, I. R. *J. Phys. Chem. B* **2001**, *105*, 7280.
- [12] Szablewski, M. *J. Org. Chem.* **1994**, *59*, 954.
- [13] Chen, B. *Ph.D. Dissertation*, The University of Alabama, **1999**.
- [14] Wang, B.; Xiao, X.; Sheng, P. *J. Vac. Sci. Technol. B* **2000**, *18*, 2351.
- [15] Reed, M. A., private communication.
- [16] Aviram, A.; Ratner, M. A. *Chem. Phys. Lett.* **1974**, *29*, 227.
- [17]. Burger, K.; Tschismarov, F.; Ebel, H. *J. Electron Spectrosc. Relat. Phenom.* **1977**, *10*, 461.
- [18] Vannerberg, N. G. *Chem. Scr.* **1976**, *9*, 122.
- [19] Hughes, T. V.; Mokijewski, B.; Chen, B.; Lakshmikantham, M. V.; Cava, M. P.; Metzger, R. M. *Langmuir* **1999**, *15*, 6925.
- [20] Inelastic Mean Free Path Database Software, National Institute of Standards and Technology Database, U.S. Department of Commerce.
- [21] Steiner, U.; Caseri, W.; Suter, U. *Langmuir*, **1992**, *8*, 2771.
- [22] Arnold, R.; Terfort, A.; Woll, C.; *Langmuir*, **2001**, *17*, 4980.
- [23] Ashwell, G. J.; Jefferies, G.; Dawnay, E.; Kuczynski, A.; Lynch, D.; Yu G.; Bucknall, D. *J. Mater. Chem.*, **1995**, *5*, 975.
- [24] Xu, T.; Szulczewski, G. J.; Morris, T. A.; Metzger, R. M. to be published.



$C_{16}H_{33}Q^+-3CNQ^-$, molecule **1**[10, 11]



$(C_{10}H_{21})_2N^+-3CNQ^-$, molecule **2**

Fig. 1. Chemical structures of zwitterionic $D^+-\pi-A^-$ molecules. For molecule **2**, the positive charge is located on the ammonium nitrogen atom and the negative charge is on the carbon atom between the two cyano groups.

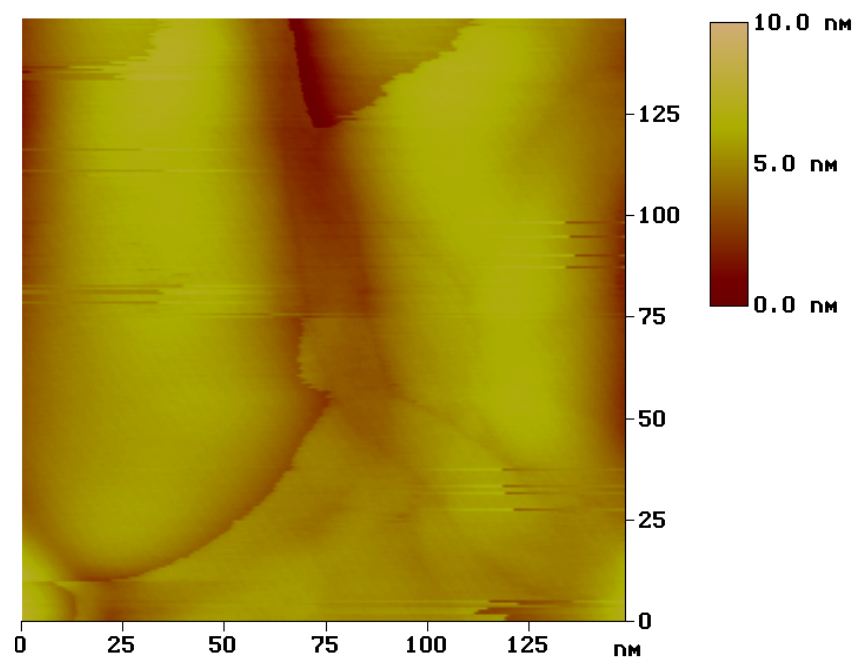


Fig.2. Typical AFM images (150nm ×150nm) of 150 nm thick gold films grown on 7 nm Ti adhesion layer on glass substrates at temperature of 260 °C.

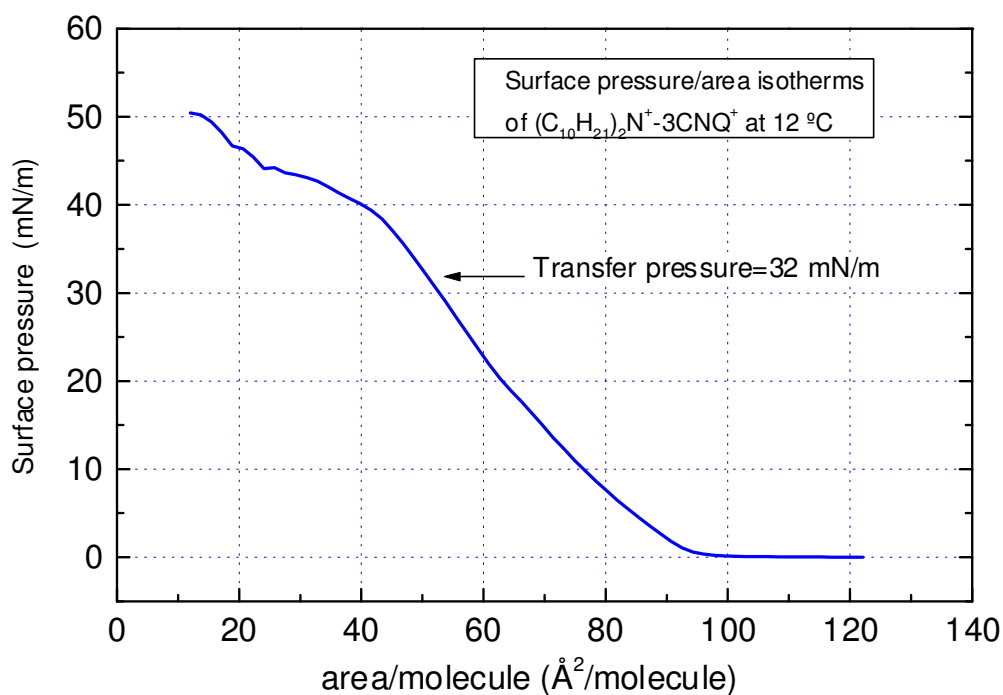


Fig.3. The surface pressure vs area isotherm. The $(C_{10}H_{21})_2N^+-3CNQ^-$ Pockels-Langmuir monolayer at air-water interface collapses at $\pi_c \approx 39-41 \text{ mN}\cdot\text{m}^{-1}$. Transfer pressure is $32 \text{ mN}\cdot\text{m}^{-1}$, which corresponds to *ca.* $50 \text{ \AA}^2 \text{ molecule}^{-1}$. The upstroke transfer ratio is slightly greater than unity.

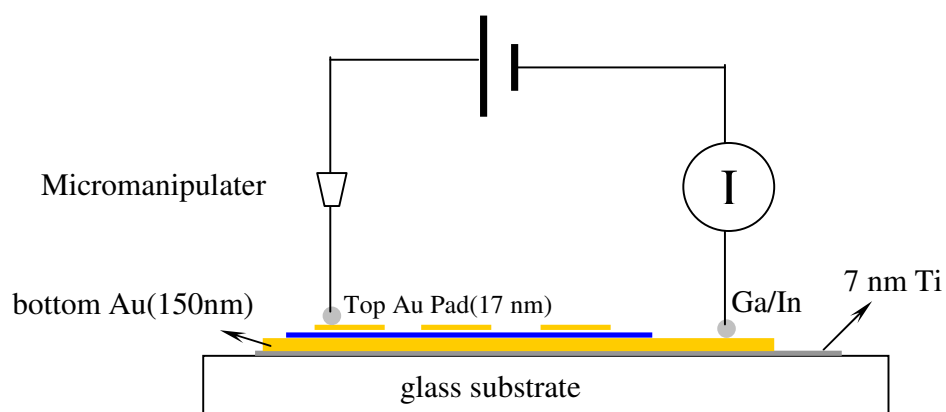


Fig. 4. Schematic diagram of LB monolayer of $(C_{10}H_{21})_2N^+-3CNQ^-$ sandwiched between Au electrodes (pad area=0.283 mm²) and electrical contacts attached to the Au electrodes.

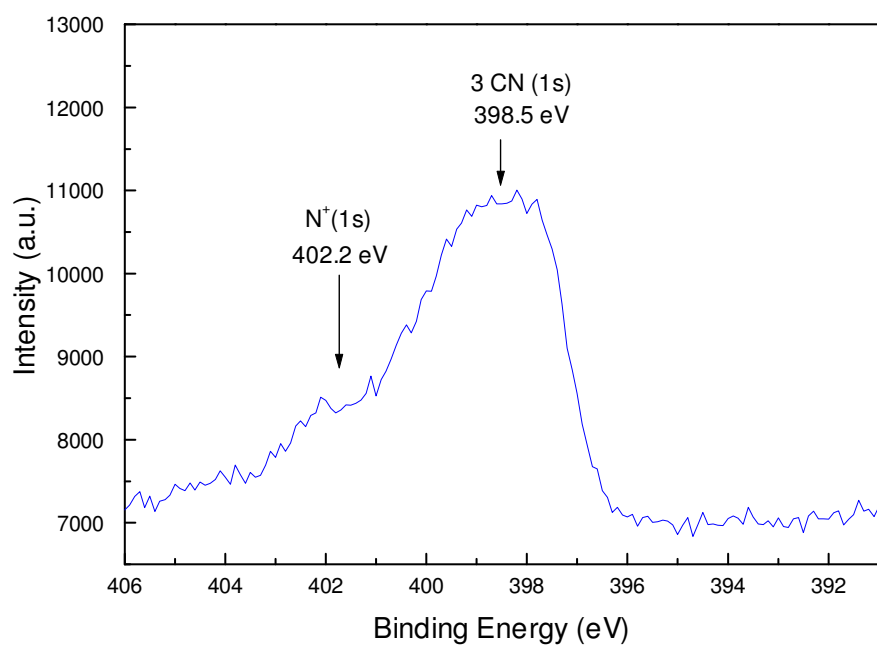


Fig. 5. High-resolution N(1s) XPS of $(\text{C}_{10}\text{H}_{21})_2\text{N}^+-3\text{CNQ}^-$ LB 12 multilayers on Au

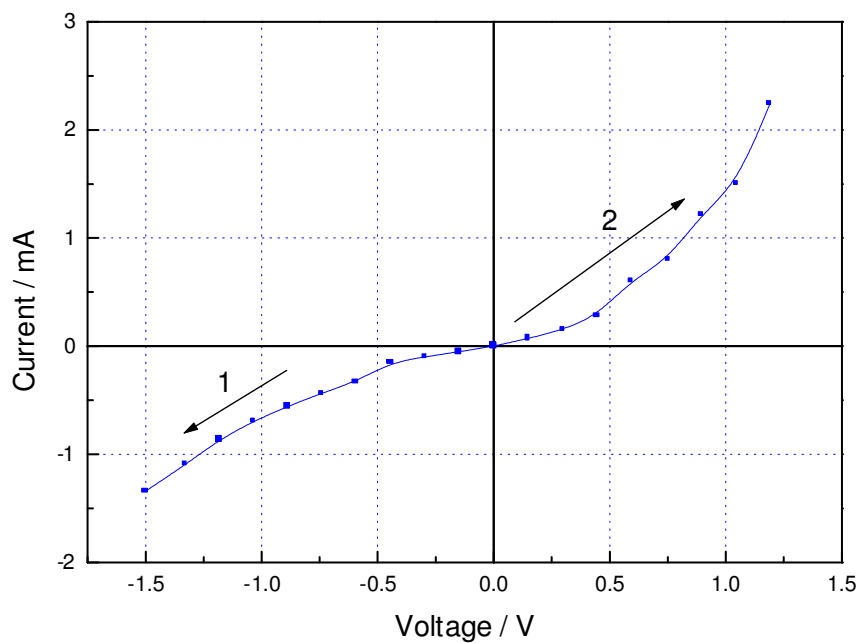


Fig.6. Current-voltage plot(I-V) for LB monolayer of $(C_{10}H_{21})_2N^+-3CNQ^-$, in cell “Au top pad | $(C_{10}H_{21})_2N^+-3CNQ^-$ monolayer | Au base”. The scanning direction is from 0 V to -1.5 V, and then from 0 V to 1.2 V. The cell undergoes short circuit at $> +1.2$ V. The nominal rectification ratio is $RR=2.2$ (at ± 1.2 V, i.e. no significant rectification).

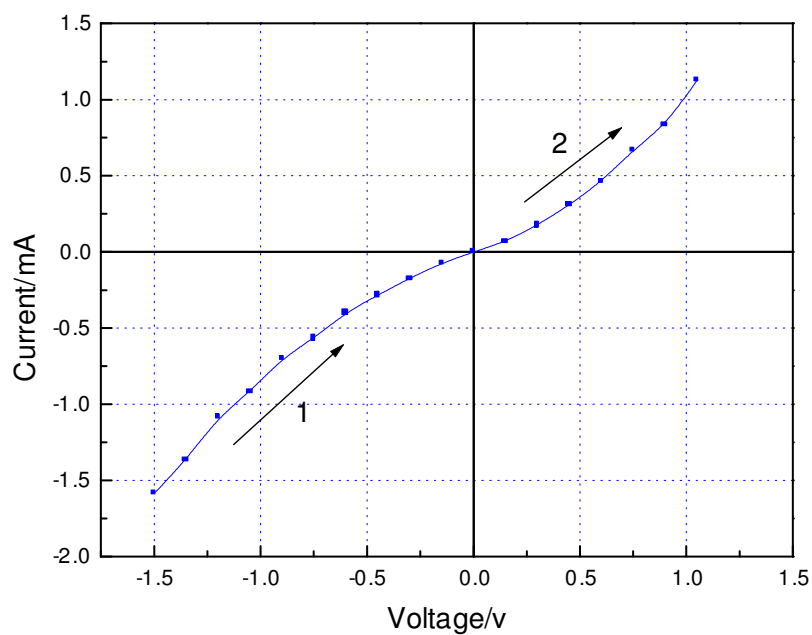


Fig. 7. Current-voltage plot(I-V) for LB monolayer of $(C_{10}H_{21})_2N^+-3CNQ^-$, in cell “Au top pad | $(C_{10}H_{21})_2N^+-3CNQ^-$ monolayer | Au base”. The scanning direction is from -1.5 V to 1.0 V, and undergoes short circuit at $> +1.0$ V. The nominal rectification ration is $RR=1$ (at ± 1.0 V, i.e. no rectification).

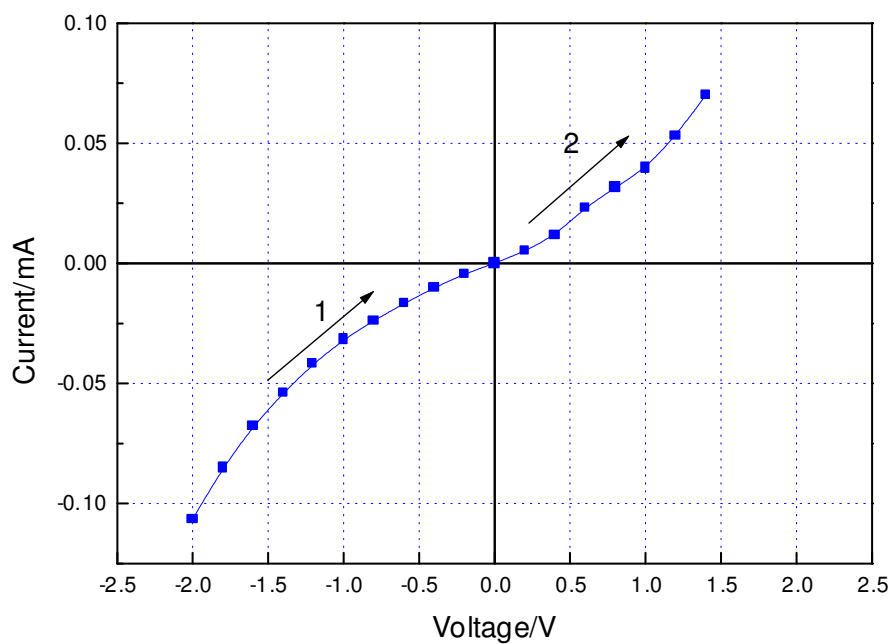


Fig. 8. Current-voltage plot(I-V) for LB monolayer of $(C_{10}H_{21})_2N^+-3CNQ^-$, in cell “Au top pad | $(C_{10}H_{21})_2N^+-3CNQ^-$ monolayer | Au base”. The scanning direction is from -2.0 V to 1.4 V, and undergoes short circuit at $> +1.4$ V. The nominal rectification ratio is $RR=1.4$ (for ± 1.4 V, i.e. there is no significant rectification).

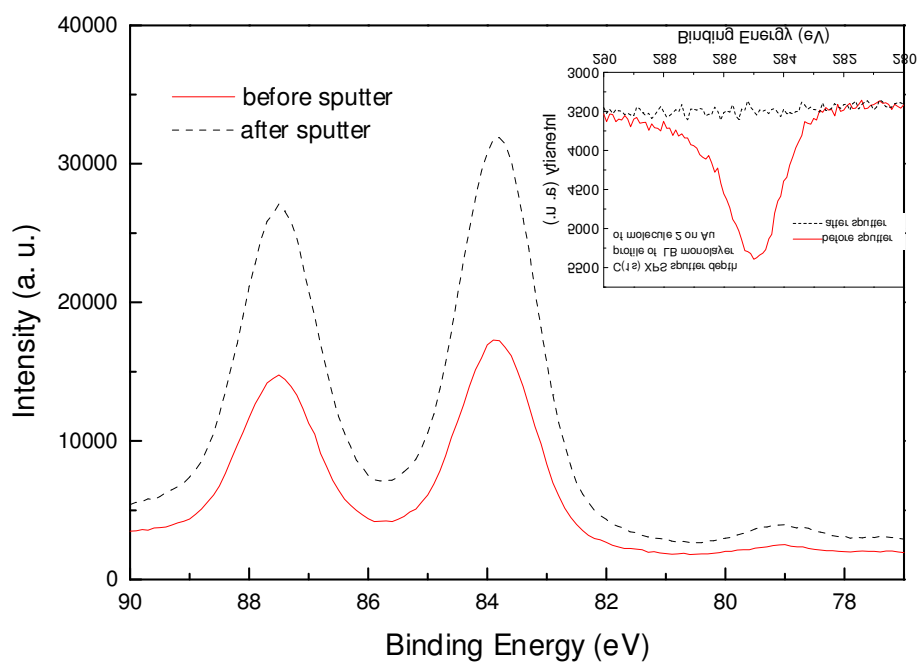


Fig. 9. XPS sputter depth profile of LB monolayer of $(C_{10}H_{21})_2N^+-3CNQ^-$ on a gold film. Inset: the C(1s) signal before and after sputtering.

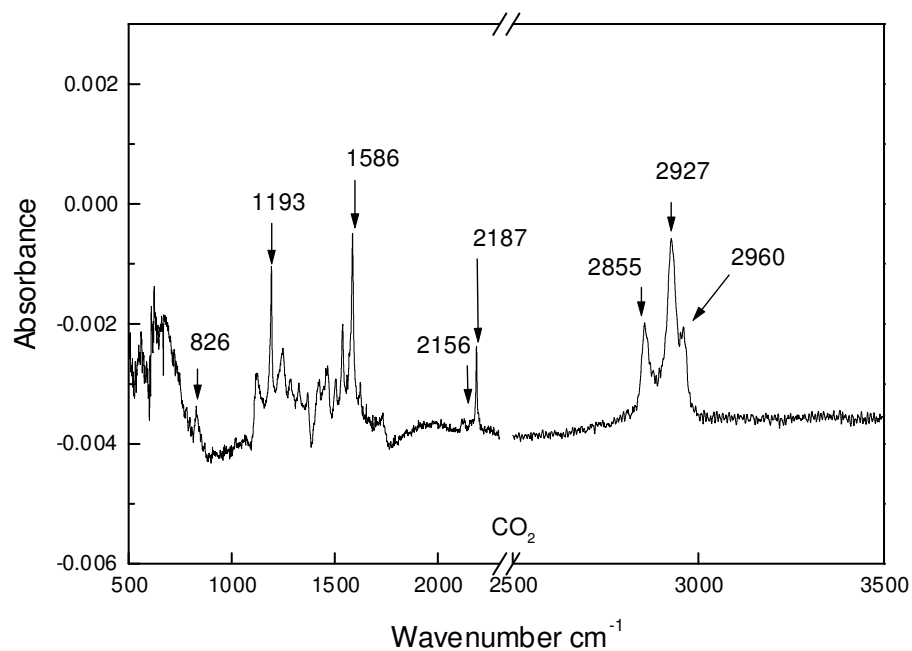


Fig.10. Reflection absorption infrared spectrum of a $(C_{10}H_{21})_2N^+-3CNQ^-$ LB monolayer on a 150 nm thick Au film.

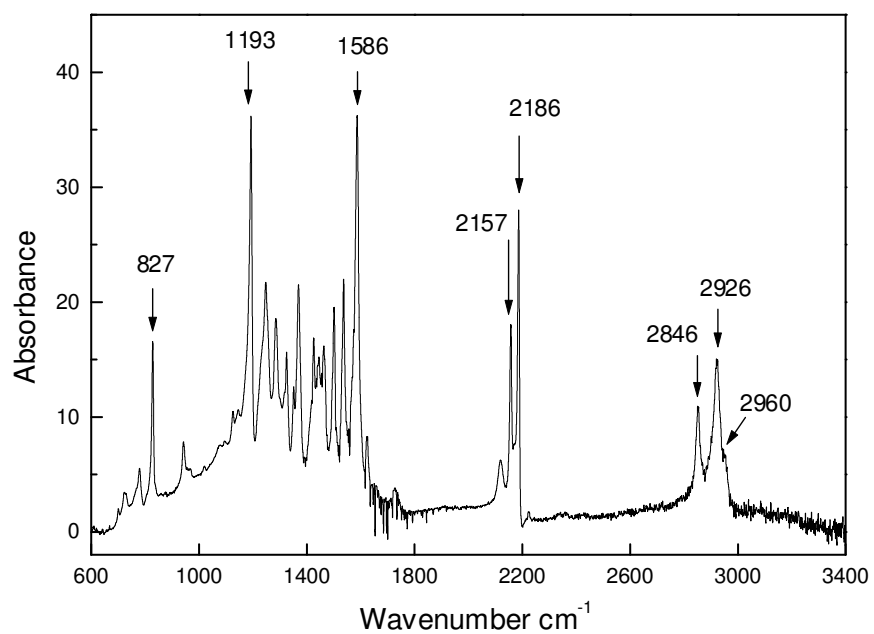
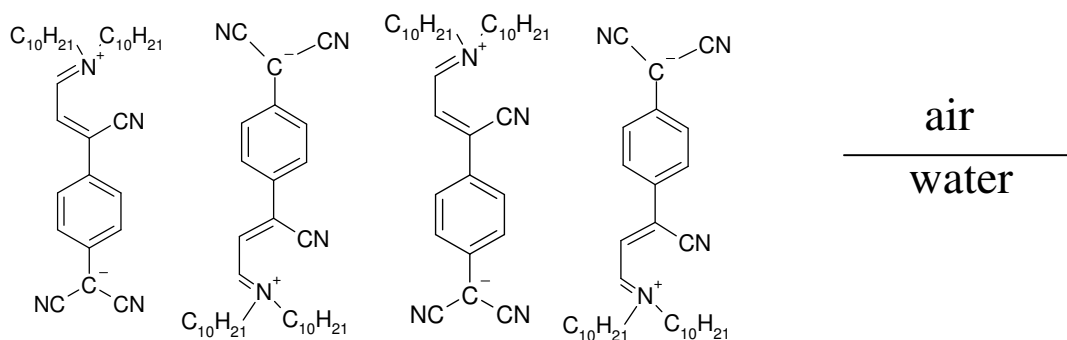
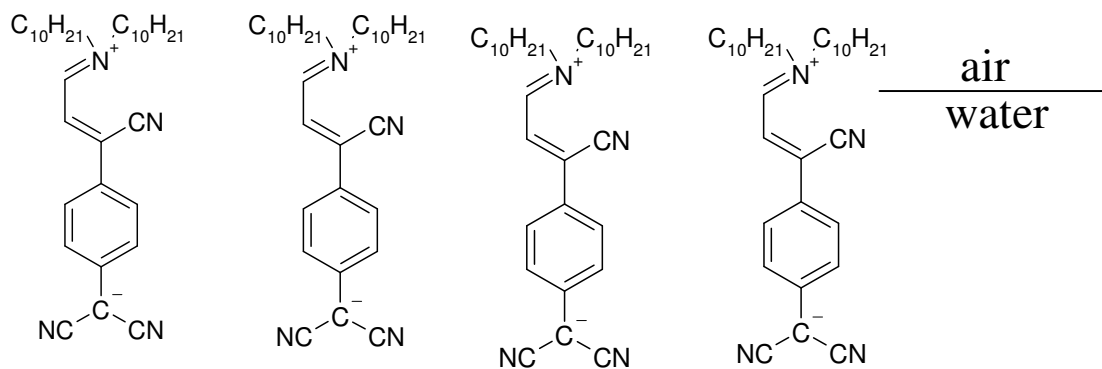


Fig. 11. Transmission infrared spectrum of bulk $(\text{C}_{10}\text{H}_{21})_2\text{N}^+-3\text{CNQ}^-$ deposited from a CH_2Cl_2 solution onto a KBr disk.



a. Dipole preferred antiparallel alignment



b. Hydrophobicity/hydrophilicity preferred parallel alignment

Fig. 12 Two competing forces may determine the molecular orientation at the air-water interface:

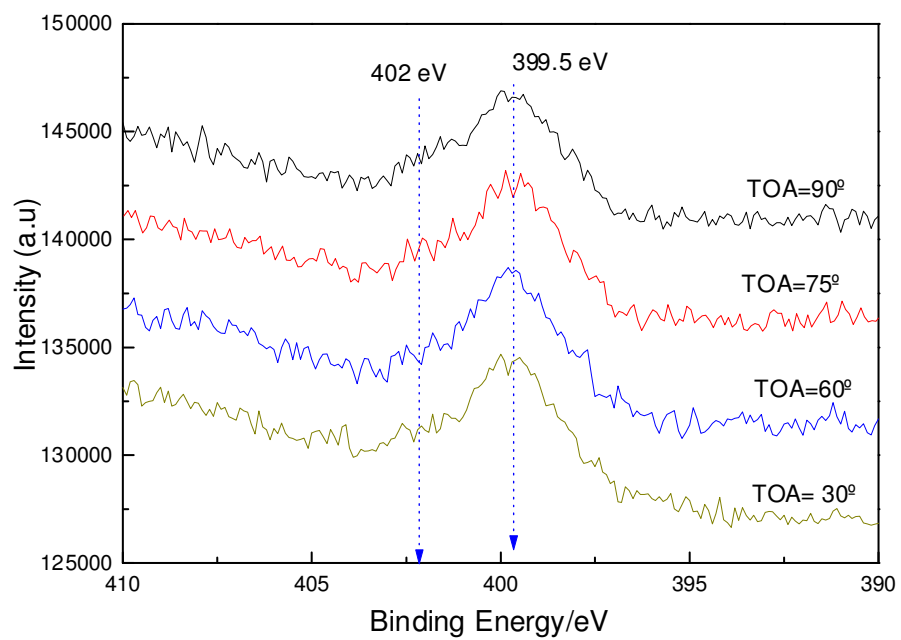


Fig. 13. N(1s) angle-resolved XPS of a $(C_{10}H_{21})_2N^+-3CNQ^-$ LB monolayer on Au.

Table 1. Assignments of IR bands of (C₁₀H₂₁)₂N⁺-3CNQ⁻ LB monolayer on gold and bulk (C₁₀H₂₁)₂N⁺-3CNQ⁻ deposited on a KBr disk.

Mode	Peak in RAIRS	Peak in Bulk IR
<i>o</i> - benzene H out-of-plane C-H vibration	826	827
C-N stretch	1193	1193
C=N stretch	1568	1568
middle C≡N stretch	2156	2157
terminal C≡N stretch	2187	2186
CH ₂ symmetric stretch	2855	2846
CH ₂ asymmetric stretch	2927	2926
CH ₃ asymmetric stretch	2961	2960